

Thin film dilute ferromagnetic semiconductors $\text{Sb}_{2-x}\text{Cr}_x\text{Te}_3$ with a Curie temperature up to 190 K

Zhenhua Zhou, Yi-Jiunn Chien, and Ctirad Uher

Department of Physics, University of Michigan, Ann Arbor, Michigan 48109, USA

(Received 30 October 2006; published 15 December 2006)

Thin film semiconductors $\text{Sb}_{2-x}\text{Cr}_x\text{Te}_3$ ($0 \leq x \leq 0.59$) based on tetradymite-type structure of Sb_2Te_3 have been prepared on the (0001) sapphire substrates by low-temperature molecular beam epitaxy. The films display ferromagnetism with the Curie temperature increasing nearly linearly with the content of Cr incorporated in the lattice. The highest Curie temperature reached so far is 190 K in a $\text{Sb}_{1.41}\text{Cr}_{0.59}\text{Te}_3$ film. Structural studies, magnetic characterization, and transport measurements indicate the robust nature of the magnetic state that has its easy axis of magnetization perpendicular to the plane of the film. The structures thus represent diluted magnetic semiconductors with a high Curie temperature and highly anisotropic properties.

DOI: [10.1103/PhysRevB.74.224418](https://doi.org/10.1103/PhysRevB.74.224418)

PACS number(s): 75.50.Pp, 72.20.-i, 75.70.-i

I. INTRODUCTION

Diluted magnetic semiconductors (DMS) with high Curie temperature are important components in new electronic devices based on semiconductor spintronics. Although extensive efforts are being devoted to the study of Mn-doped GaAs,¹⁻³ transition metal (TM)-doped GaN,^{4,5} and Cr-doped ZnTe (Ref. 6) semiconductors, investigations of new DMSs based on other host semiconductors are also attracting much attention. Among them, DMSs based on tetradymite-type $A_2^{\text{VI}}B_3^{\text{VI}}$ ($A=\text{Bi}, \text{Sb}; B=\text{Te}$) semiconductors are of particular interest since they permit investigations of the influence of the partially filled $3d$ shells of TM in the highly anisotropic matrix of Sb_2Te_3 rather than in the zinc blende structure. Sb_2Te_3 and Bi_2Te_3 are narrow band gap semiconductors with the tetradymite-type layered structure. They are characterized by octahedral bonding and a van der Waals gap that separates five atom layer lamellae $\text{Te}^{(1)}\text{-A-Te}^{(2)}\text{-A-Te}^{(1)}$. The bonding is primarily ionic and covalent within the layers $\text{Te}^{(1)}\text{-A}$ and $\text{A-Te}^{(2)}$, and van der Waals forces act between the Te double layers $\text{Te}^{(1)}\text{-Te}^{(1)}$.⁷ Sb_2Te_3 and Bi_2Te_3 with stoichiometric composition are diamagnetic. It was found recently that bulk single crystals of several TM-doped Sb_2Te_3 and Bi_2Te_3 , namely, $\text{Sb}_{2-x}\text{V}_x\text{Te}_3$,⁸ $\text{Sb}_{2-x}\text{Cr}_x\text{Te}_3$,⁹ and $\text{Bi}_{2-x}\text{Fe}_x\text{Te}_3$ (Ref. 10) support ferromagnetism with the Curie temperature of 22 K ($x=0.03$), 20 K ($x=0.095$), and 12 K ($x=0.08$), respectively. The values of x indicated in the parentheses represent the highest content of TM that can be substituted on the Sb and Bi sublattices of bulk single crystals of Sb_2Te_3 and Bi_2Te_3 prepared by the Bridgman growth technique. Attempts to incorporate higher concentrations of TM resulted in a segregation of the second phase and a visible deterioration of the otherwise perfect single-crystalline samples.

To overcome the limitations imposed by the low solubility of TM in the bulk matrices of Sb_2Te_3 and Bi_2Te_3 , we have made use of low-temperature molecular beam epitaxy technique to grow thin films of TM-doped Sb_2Te_3 . In our initial attempt with vanadium we demonstrated^{11,12} that the solubility of TM was dramatically enhanced and we were able to fabricate well oriented films of $\text{Sb}_{2-x}\text{V}_x\text{Te}_3$ with x up to 0.35. With the much enhanced content of vanadium, the films dis-

played ferromagnetism to temperatures of 177 K. This success encouraged us to explore the possibility of enhancing the solubility of Cr in Sb_2Te_3 and thus increasing the Curie temperature of the $\text{Sb}_{2-x}\text{Cr}_x\text{Te}_3$ films. This paper describes the outcome of the study.

II. EXPERIMENTS

Thin films of $\text{Sb}_{2-x}\text{Cr}_x\text{Te}_3$ with x up to 0.59 were grown in our MBE system by coevaporating Sb, Te, and Cr onto sapphire (0001) substrates held at 312 °C. Sb and Te were evaporated using Knudsen cells while Cr was deposited with the aid of a miniature e gun. The growth rate of all films was kept at 1.9–2.0 Å/s and we used a fixed flux ratio (Sb, Cr): Te=1:4 found by trial and error to yield the tetradymite-type Sb_2Te_3 structure with the correct stoichiometry. The deposition rates and overall thickness of the films (typically 0.15 μm) were controlled by calibrated quartz-crystal monitors. Streaklike reflection high energy electron diffraction (RHEED) pattern indicates a near layer-by-layer growth of the films on (0001) sapphire even though the lattice mismatch (11%) is rather severe. The films were subsequently analyzed by x-ray diffraction and electron microprobe analysis (EPMA) to confirm their tetradymite-type crystal structure, film orientation, stoichiometry, and the content and homogeneity of Cr. Magnetization measurements were done in a quantum design SQUID-based magnetometer equipped with a 5.5 T magnet. Great care was taken when extracting the magnetization data of the film samples. Magnetization of the sapphire substrate as well as of the plastic straw holder was measured separately and their respective contributions were subtracted from the raw data. Electrical resistivity and the Hall effect were measured using an ac bridge with 16 Hz excitation, the current was injected parallel to the film plane and the magnetic field was oriented perpendicular to the film.

III. RESULTS

A series of $\text{Sb}_{2-x}\text{Cr}_x\text{Te}_3$ films has been prepared spanning x up to 0.59. The composition of the $\text{Sb}_{2-x}\text{Cr}_x\text{Te}_3$ films was determined by averaging 30 measurements taken at randomly selected locations on each film. The EPMA maps in-

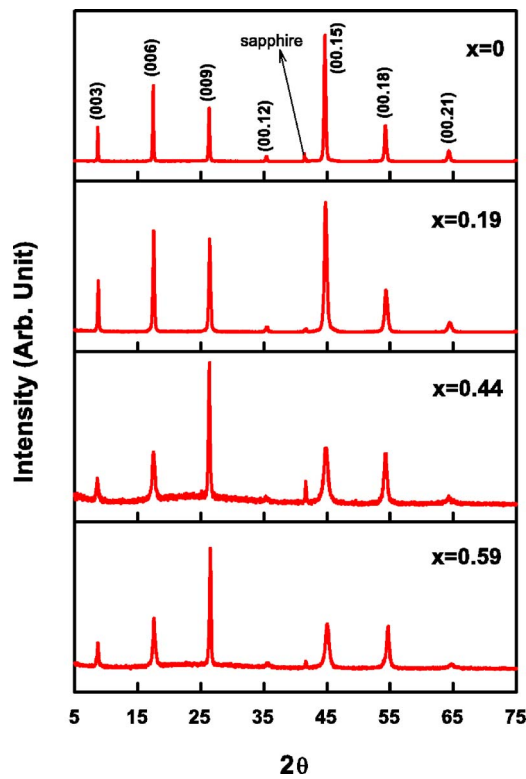


FIG. 1. (Color online) X-ray diffraction patterns of $\text{Sb}_{2-x}\text{Cr}_x\text{Te}_3$ films on sapphire (0001) substrates.

dedicate a homogeneously distributed Cr without any tendency to cluster at least on the scale of the instrument resolution. Figure 1 shows the x-ray diffraction pattern of $\text{Sb}_{2-x}\text{Cr}_x\text{Te}_3$ films. Except for sapphire substrate peaks observed in the XRD pattern, only (00.n) reflections in the hexagonal unit cell are present, confirming that the films grow parallel to the c -axis direction. No trace of any secondary phase formation was found from the XRD scans. In Fig. 2 is plotted the dependence of the lattice constants a and c of $\text{Sb}_{2-x}\text{Cr}_x\text{Te}_3$ films respectively determined from the RHEED and XRD patterns as a function of chromium concentration x . The a -axis lattice constant decreases with the increasing concentration of chromium. The c -axis lattice constant also decreases with the increasing chromium content but the percentage change is much smaller. Overall, the hexagonal unit cell of the films decreases with the increasing x . In principle, impurity atoms can be incorporated into the Sb_2Te_3 crystal lattice by the following distinct processes: by substituting for the cation (Sb) or anion (Te), by occupying interstitial lattice sites, and by entering the van der Waals gaps. Given the formal ionic radii of Sb^{3+} (0.90 Å) and Te^{2-} (2.07 Å) in the octahedral coordination of the tetradymite structure and the ionic radii of various Cr ions [Cr^{2+} (0.87 Å), Cr^{3+} (0.76 Å), Cr^{4+} (0.69 Å)], it is clear that Cr cannot occupy the anion sites. If Cr occupied interstitial positions or was located in the van der Waals gap, large lattice expansion would ensue and this is not observed. Moreover, weak bonding of Cr in such positions would likely lead to a stripping of its electrons and thus a decrease in the density of holes. As we discuss in the following section, the exactly opposite trend is

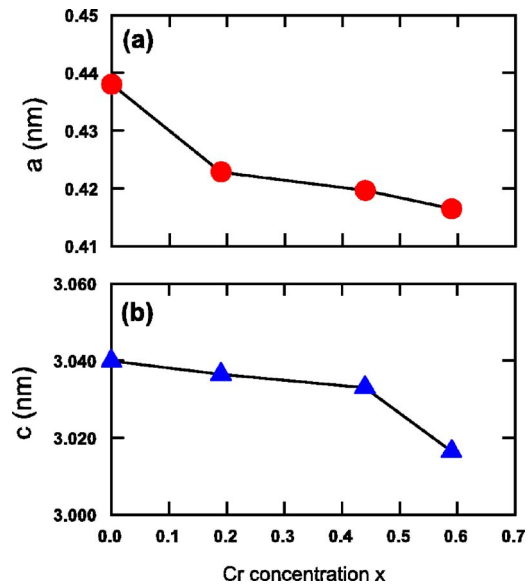


FIG. 2. (Color online) Lattice constants of $\text{Sb}_{2-x}\text{Cr}_x\text{Te}_3$ films as a function of Cr concentration x .

observed—the density of holes increases modestly as more Cr is incorporated in the crystal lattice. Thus, the above considerations suggest that Cr substitutes on the Sb sublattice just as was the case of Cr in bulk single crystals of Sb_2Te_3 .⁹ This conclusion is also strongly supported by the Cr magnetization analysis discussed later on in this paper.

Figure 3(a) shows the temperature dependent magnetization of several films of $\text{Sb}_{2-x}\text{Cr}_x\text{Te}_3$ with a progressively increasing content of Cr. The data were taken in the magnetic field of 100 Oe applied perpendicular to the plane of the films upon cooling from 300 K down to 2 K. When the temperature is lowered below 200 K, the initial very small and nearly constant magnetization at high temperatures undergoes a sharp upturn, indicated by arrows in Fig. 3(a). The sample with the highest content of Cr ($x=0.59$) has the highest onset temperature and the samples with the lower concentration of Cr show upturns at progressively lower temperatures. In comparison, pure Sb_2Te_3 displays a weakly diamagnetic behavior and on the scale of Fig. 3(a) its trace overlaps with the baseline with no hint of any upturn down to 2 K. The upturns on the magnetization curves of Cr-doped Sb_2Te_3 films indicate the onset of long-range magnetic ordering (ferromagnetism) in the films. We have used Arrott plots to pinpoint the value of the Curie temperature since the effect of magnetic anisotropy and domain rotation can be minimized.^{6,13} The Curie temperatures are shown in Fig. 4(a) as a function of Cr concentration x . A nearly linear increase of the Curie temperature with increasing concentration of Cr is observed. Currently, the maximum Curie temperature is 190 K for the film $\text{Sb}_{1.41}\text{Cr}_{0.59}\text{Te}_3$. Our data suggest that even higher values of the ordering temperature may be possible if one can further increase the concentration of Cr.

Figure 3(b) shows the temperature dependence of the electrical resistivity of the same films. The resistivity of an undoped Sb_2Te_3 film shows a typical semiconducting behavior with a negative coefficient of temperature dependence. This is different from bulk single crystals of Sb_2Te_3 which

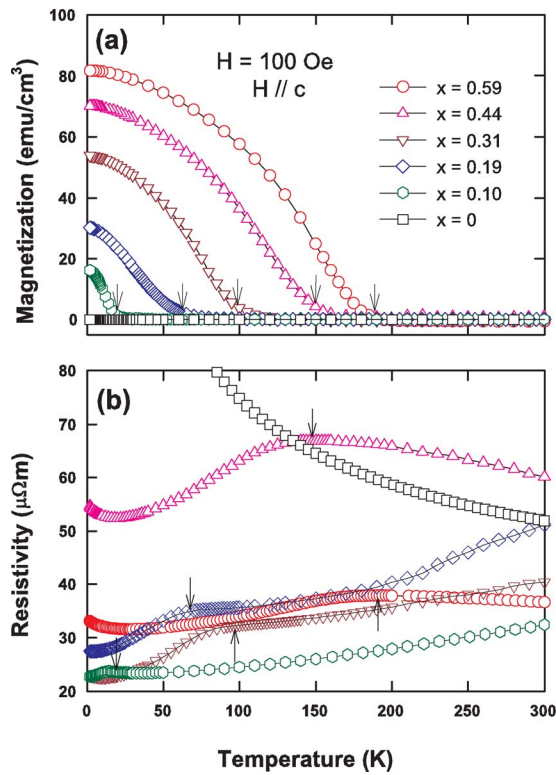


FIG. 3. (Color online) (a) Temperature dependent magnetization of $\text{Sb}_{2-x}\text{Cr}_x\text{Te}_3$ thin films. (b) Electrical resistivity of $\text{Sb}_{2-x}\text{Cr}_x\text{Te}_3$ films in zero magnetic field.

usually have a positive coefficient of temperature dependence characteristic of a degenerate semiconductor. Such difference is mainly due to the different carrier concentrations in Sb_2Te_3 single crystals and Sb_2Te_3 films. Typical carrier concentration in Sb_2Te_3 single crystals and Sb_2Te_3 film are 10^{20} cm^{-3} and $5.2 \times 10^{19} \text{ cm}^{-3}$,¹¹ respectively, reflecting different concentrations of antisite defects of the type Sb_{Te} (i.e., antimony located on the site of Te). All curves of resistivity vs. temperature of Cr-doped films show a local maximum (hump) around T_C , which moves to higher temperatures with the increasing concentration of Cr. Such behavior of the resistivity is the result of spin-disorder scattering that sets in at the paramagnetic-to-ferromagnetic transition;^{14,15} in other words, it indicates the magnetic ordering temperature of the films. The temperatures at which the resistivity reaches the local maximum are marked with arrows in Fig. 3(b). It can be seen that these temperatures correspond very well to the magnetic onset temperatures in Fig. 3(a). While $\text{Sb}_{2-x}\text{Cr}_x\text{Te}_3$ films with low Cr content ($x \leq 0.31$) show metallic character of resistivity, (except at very low temperatures where a slight upturn is observed), the two films with high content of Cr ($x = 0.44$ and $x = 0.59$) show a negative temperature coefficient in their paramagnetic domain, i.e., the films undergo a metal-insulator transition as a function of Cr concentration. These two films also display more pronounced upturns at the lowest temperatures. Below the magnetic ordering temperatures, all resistivity curves show similar temperature dependences characterized by a decreasing resistivity before a minimum is reached at temperatures varying from 29 K down to 2.5 K, the lower temperature corresponding to the lower Cr concen-

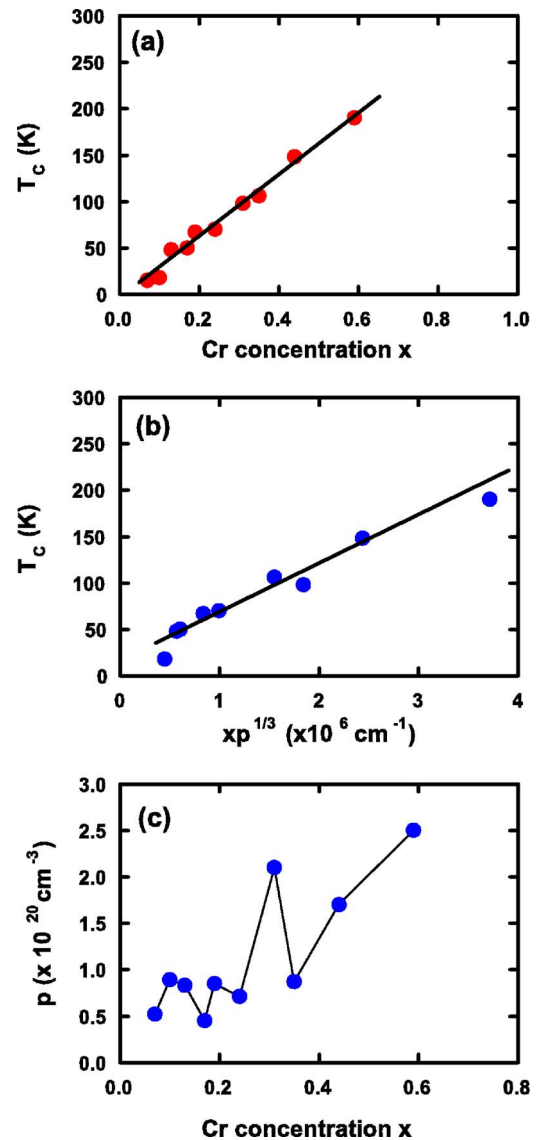


FIG. 4. (Color online) Curie temperature of $\text{Sb}_{2-x}\text{Cr}_x\text{Te}_3$ thin films as a function of (a) Cr concentration x , (b) $xp^{1/3}$. (c) Room temperature hole concentration as a function of Cr content x .

tration. It is not clear whether the upturns at very low temperatures arise as a consequence of localization or are a signature of the carrier freeze out. Dyck *et al.*⁹ and Kulbachinskii *et al.*¹⁶ studied the temperature dependence of the resistivity of Cr-doped Sb_2Te_3 bulk single crystals and their results indicated metallic behavior. The Cr concentration x in their bulk crystalline samples is less than 0.1 and in this range of concentrations our data on Cr-doped Sb_2Te_3 films are in good agreement with the bulk Cr-doped Sb_2Te_3 crystals. We note that impurity concentration dependent metal-insulator transition was also observed in Mn-doped GaAs.^{17,18}

Room temperature hole concentration was obtained through Hall coefficient measurements. Since at 300 K all films are in their paramagnetic phase, there is no complication with an anomalous Hall effect contribution and the carrier density can be unambiguously determined assuming that a single band model adequately describes the carrier spec-

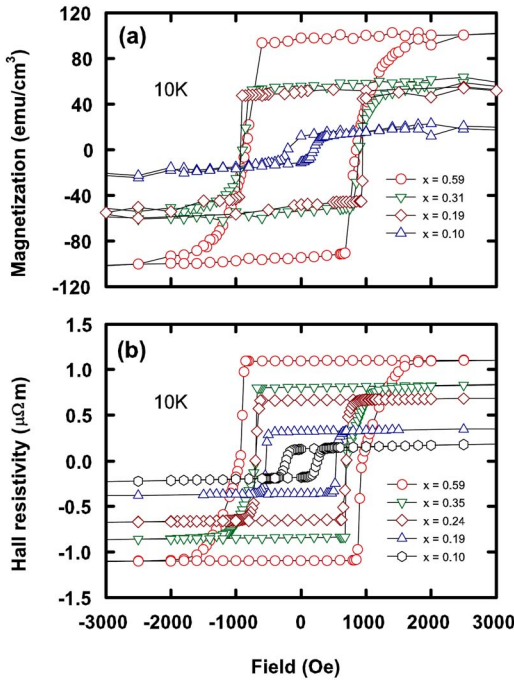


FIG. 5. (Color online) (a) Magnetic hysteresis loops of $\text{Sb}_{2-x}\text{Cr}_x\text{Te}_3$ thin films. (b) Magnetic field dependent Hall resistivity of $\text{Sb}_{2-x}\text{Cr}_x\text{Te}_3$ films.

trum. Unlike in Bi_2Te_3 where the intrinsic conduction starts to contribute at ambient temperatures, the gap in Sb_2Te_3 is larger (0.26 eV) and the intrinsic effects do not enter the picture at 300 K. Figure 4(c) shows the hole concentration as a function of Cr content. Overall, the concentration of holes increases modestly with the Cr content. The actual hole concentration in each film is also influenced by the density of antisite defects, i.e., the particular nonstoichiometry that reflects the growth conditions and perhaps even by the interaction of these native defects with the Cr ions.

Ferromagnetism in our $\text{Sb}_{2-x}\text{Cr}_x\text{Te}_3$ films was confirmed by field dependence of the magnetization. Figure 5(a) shows the magnetic hysteresis loops obtained at 10 K for several films with various content of Cr. The value of the coercive field is about 200 Oe for a film with $x=0.1$ and this value increases to 850 Oe when the Cr concentration increases to $x=0.59$. Smooth hysteresis loops indicate a well-ordered ferromagnetic structure and coherent rotation of spins in the films. Equally robust and well developed hysteresis loops were observed on other Cr-doped Sb_2Te_3 films except that their coercive fields and critical temperatures were different corresponding to the different content of Cr. The ferromagnetic state in $\text{Sb}_{2-x}\text{Cr}_x\text{Te}_3$ films was further confirmed by anomalous Hall effect measurements. Figure 5(b) shows the magnetic field dependent Hall resistivity of $\text{Sb}_{2-x}\text{Cr}_x\text{Te}_3$ films at 10 K. The Hall resistivity was measured with the field parallel to the c axis and the excitation current applied perpendicular to the c axis. The Hall resistivity in magnetic materials is expressed as: $\rho_H = R_0 B + R_M M$, where R_0 is the ordinary Hall coefficient, B is the magnetic field, R_M is the anomalous Hall coefficient, and M is the magnetization of the sample. While the ordinary Hall effect dominates at high

fields, as seen by the linear dependence of ρ_H with B , the anomalous Hall effect dominates at low fields due to the contribution from the magnetization. Hysteresis loops in the Hall effect are detectable to within a couple of degrees of T_C .

IV. DISCUSSION

It is evident that the films of $\text{Sb}_{2-x}\text{Cr}_x\text{Te}_3$ display robust ferromagnetism. Moreover, as Fig. 4(b) indicates, the plot of the Curie temperature is proportional to $x p^{1/3}$ where x is the impurity concentration and p is the density of holes. This might suggest that the well-known Ruderman-Kittel-Kasuya-Yoshida (RKKY) interaction is at play^{19,20} and the films thus represent an example of a diluted magnetic semiconductor (DMS). However, as with essentially all DMSs, a question arises regarding a possible formation of clusters or precipitate phases that might be the source of the long-range magnetic order instead of the uniformly distributed ions on the Sb sublattice. At this stage, we do not have available a detailed structural information such as, e.g., high resolution transmission electron micrographs. Furthermore, as Fig. 4(c) indicates, the dependence of the carrier (hole) density on the concentration of Cr ions is rather weak and the Curie temperature is dominated by its dependence on the Cr content x rather than its dependence on the charge carrier density p . These are clearly issues that make the case for the RKKY interaction and the diluted character of these magnetic semiconductor films debatable. Nevertheless, there are also features that are supportive of the notion that these films are diluted magnetic semiconductors.

From the high field-saturation magnetization (M_S) done at 10 K, the number of Bohr magnetons per Cr ion in the $\text{Sb}_{2-x}\text{Cr}_x\text{Te}_3$ films can be estimated by M_S/N , where N is the number of Cr ions determined by EPMA. Our calculations give the values of the number of Bohr magnetons per Cr ion as $3.04 \mu_B$, $2.97 \mu_B$, $3.00 \mu_B$, and $2.86 \mu_B$, for $x=0.10$, 0.24 , 0.35 , 0.59 , respectively. Overall, the values are very close to $3 \mu_B$ across the entire spectrum of Cr concentrations, including low concentrations of Cr in bulk single crystals, and indicate three unpaired spins all pointing in the same direction, i.e., the spin only value of $S=3/2$. Thus, there is a strong and consistent evidence for the valence state of Cr being $3+$ as it substitutes for the formally Sb^{3+} ion on the antimony sublattice. It should be pointed out that the $3+$ valence of antimony is merely a formal designation for Sb-Te bonding in Sb_2Te_3 which in reality is not purely ionic but has a substantial covalent character as well. The apparently isoelectronic substitution of Cr for Sb is the main reason why one observes a rather weak charge carrier (hole) dependence on the content of Cr. Nevertheless, the overall fivefold increase in the density of holes is detected, Fig. 4(c), and this just might be enough to support the RKKY interaction mechanism. Had the films contained impurity phases such as CrTe , Cr_3Te_4 , or Cr_2Te_3 that are known to be ferromagnetic with saturation moments around 2.0 – $2.7 \mu_B$ and the Curie temperatures ranging from 180 K to 340 K, we would not observe a linearly dependent variation of T_C on the concentration of Cr nor the smooth hysteresis loops.

V. CONCLUSIONS

In summary, by making use of low-temperature molecular beam epitaxy, we have been able to dramatically extend the range of solubility of Cr in Sb_2Te_3 and prepared well-oriented $\text{Sb}_{2-x}\text{Cr}_x\text{Te}_3$ films with x up to 0.59. The films possess high Curie temperature that increases linearly with the content of Cr and reaches 190 K in the film of $\text{Sb}_{1.41}\text{Cr}_{0.59}\text{Te}_3$. The ferromagnetic state was confirmed by hysteresis in the magnetization and by the presence of the anomalous Hall effect. Magnetization analysis indicates that Cr substitutes on the antimony sublattice and attains the valence state of 3+, just as was the case in bulk single crystals. The resulting relatively weak dependence of the density of

holes on the content of Cr brings into question the applicability of the RKKY interaction. On the other hand, the linearly varying Curie temperature and smooth hysteresis loops suggest that the system is consistent with the behavior of a diluted magnetic semiconductor. The preferentially perpendicular orientation of magnetic spins in the films of $\text{Sb}_{2-x}\text{Cr}_x\text{Te}_3$ makes the system of potential interest for ultra-high density perpendicular magnetic recording.

ACKNOWLEDGMENT

This work was supported by National Science Foundation Grant No. NSF-DMR-0305221 and No. NSF-DMR-0604549.

-
- ¹H. Ohno, A. Shen, F. Matsukura, A. Oiwa, A. Endo, S. Katsumoto, and Y. Iye, *Appl. Phys. Lett.* **69**, 363 (1996).
²H. Ohno, *J. Magn. Magn. Mater.* **200**, 110 (1999).
³K. W. Edmonds, K. Y. Wang, R. P. Campion, A. C. Neumann, N. R. S. Farley, B. L. Gallagher, and C. T. Foxon, *Appl. Phys. Lett.* **81**, 4991 (2002).
⁴S. Sonoda, S. Shimiza, T. Sasaki, Y. Yamamoto, and H. Hori, *J. Cryst. Growth* **237-239**, 1358 (2002).
⁵M. E. Overberg, C. R. Abernathy, S. J. Pearton, N. A. Theodoropoulou, K. T. McCarthy, and A. F. Hebard, *Appl. Phys. Lett.* **79**, 1312 (2001).
⁶H. Saito, V. Zayets, S. Yamagata, and K. Ando, *Phys. Rev. Lett.* **90**, 207202 (2003).
⁷H. Scherrer and S. Scherrer, in *CRC Handbook of Thermoelectrics*, edited by D. M. Rowe (Chemical Rubber, Boca Raton, FL, 1995), p. 211.
⁸J. S. Dyck, P. Hájek, P. Lošťák, and C. Uher, *Phys. Rev. B* **65**, 115212 (2002).
⁹J. S. Dyck, Č. Drašar, P. Lošťák, and C. Uher, *Phys. Rev. B* **71**, 115214 (2005).
¹⁰V. A. Kulbachinskii, A. Yu. Kaminskii, K. Kindo, Y. Narumi, K. Suga, P. Lošťák, and P. Švanda, *JETP Lett.* **73**, 352 (2001).
¹¹Y.-J. Chien, Z. Zhou, and C. Uher, *J. Cryst. Growth* **283**, 309 (2005).
¹²Z. Zhou, Y.-J. Chien, and C. Uher, *Appl. Phys. Lett.* **87**, 112503 (2005).
¹³A. Arrott, *Phys. Rev.* **108**, 1394 (1957).
¹⁴S. von Molnar and T. Kasuya, *Phys. Rev. Lett.* **21**, 1757 (1968).
¹⁵T. Kasuya, *Prog. Theor. Phys.* **16**, 45 (1956).
¹⁶V. A. Kulbachinskii, P. M. Tarasov, and E. Brueck, *Physica B* **368**, 32 (2005).
¹⁷F. Matsukura, H. Ohno, A. Shen, and Y. Sugawara, *Phys. Rev. B* **57**, R2037 (1998).
¹⁸A. Oiwa, S. Katsumoto, A. Endo, M. Hirasawa, Y. Iye, H. Ohno, F. Matsukura, A. Shen, and Y. Sugawara, *Solid State Commun.* **103**, 209 (1997).
¹⁹T. Jungwirth, W. A. Atkinson, B. H. Lee, and A. H. MacDonald, *Phys. Rev. B* **59**, 9818 (1999).
²⁰C. H. Ziener, S. Glutsch, and F. Bechstedt, *Phys. Rev. B* **70**, 075205 (2004).